Extracellular vesicles secreted by *Brugia malayi* microfilariae modulate the melanization pathway in the mosquito host

Hannah J. Loghry[1], Hyeogsun Kwon[2], Ryan C Smith[2], Noelle A Sondjaja[1], Sarah J Minkler[1], Sophie Young[1], Nicolas J Wheeler[3] , Mostafa Zamanian[3], Lyric C Bartholomay[3], Michael J Kimber[1]

[1]Department of Biomedical Sciences, College of Veterinary Medicine, Iowa State University, Ames, Iowa, USA

[2]Department of Entomology, College of Agriculture and Life Sciences, Iowa State University, Ames, Iowa, USA

[3]Department of Pathobiological Sciences, College of Veterinary Medicine, University of Wisconsin-Madison, Madison, Wisconsin, USA

Abstract

Vector-borne, filarial nematode diseases represent a significant and affecting disease burden in humans, domestic animals, and livestock worldwide. Parasitic filarial nematodes require both an intermediate (vector) host and a definitive (mammalian) host during the course of their life cycle. In either host, the nematode must evade the host elicited immune response in order to develop and establish infection. There is direct evidence of parasite-derived immunomodulation in mammals, however, there is less evidence of parasite immunomodulation of the vector host. We have previously reported that all life stages of *Brugia malayi*, a causative agent of lymphatic filariasis, secrete extracellular vesicles (EVs). Here we investigate the immunomodulatory effects of microfilariae derived EVs on the vector host *Aedes aegypti*. RNA-seq analysis of an *A. aegypti* cell line treated with *B. malayi* microfilariae EVs showed differential expression of both mRNAs and miRNAs, some with roles in immune regulation. One downregulated gene, AAEL002590, identified as a serine protease, was shown to have direct involvement in the phenoloxidase (PO) cascade through analysis of PO activity. Similarly, injection of adult female mosquitoes with *B. malayi* microfilariae EVs validated these results *in vivo*, eliciting a downregulation of the AAEL002590 transcript and a significant reduction in PO activity. Our data indicates that parasite-derived EVs are capable of interfering with critical immune responses in the vector host, particularly immune responses such as melanization that target extracellular parasites. In addition, this data provides novel targets for transmission control strategies for LF and other parasitic diseases.

Author Summary

Vector-borne, filarial nematode diseases represent a significant and affecting disease burden in humans, domestic animals and livestock worldwide. Parasitic nematodes must evade the elicited immune response of their hosts in order to develop and establish infection. While there is evidence for immunomodulation of the mammalian host, the mechanism of this immunomodulation is not fully clear and there is limited evidence for immunomodulation of the vector host. Here we have shown that parasite-derived extracellular vesicles are effector structures for immunomodulation of the vector host. In particular, we have identified that parasite-derived extracellular vesicles can interfere with critical mosquito immune responses against parasites. This data provides insight into parasite biology and novel targets for transmission control strategies for parasitic diseases.

1. Introduction

Vector-borne, filarial nematode diseases represent a significant and affecting disease burden in humans, domestic animals, and livestock worldwide. In humans, Lymphatic Filariasis (LF) is caused by multiple species of filarial nematodes, including *Brugia malayi* and is endemic in 72 countries with over 860 million people infected or at risk of infection (1). Adult parasites reside in the lymphatic vasculature and although often asymptomatic, infection can result in extreme morbidity including lymphangitis, lymphedema (primarily in the extremities), and secondary bacterial infection/dermatitis (2). Current control strategies rely on mass drug administration programs that utilize inadequate anthelmintic drugs that do not effectively kill adult parasites or resolve established infections. The need for new control strategies of filarial nematode diseases is

necessary, however, progress in developing effective treatments has been stalled by our lack of understanding of parasite biology and host-parasite interactions.

Parasitic filarial nematodes require both an intermediate (vector) host and a definitive (mammalian) host during the course of their life cycle. In either host, the nematode must evade the elicited immune response of the host in order to develop and establish infection. Various immune evasion strategies have been documented, including manipulation of host immune responses (3). In mammals, there is direct evidence of parasite-derived immunomodulation. It has been shown that parasites are capable of expanding regulatory immune cells (4–10), inducing apoptosis in type 1 immune response cell types (11–14), manipulating pattern recognition receptors (PRRs) (15–21), and increasing anti-inflammatory cytokines such as IL-4/IL-10 (22–24). However, there is less extensive evidence of parasite immunomodulation of the vector host. Early studies have shown that filarial nematode parasites can inhibit melanization (25). Melanotic encapsulation, a crucial mosquito innate immune response to the microscopic larval stages of the parasite that infect mosquitoes, is a core arthropod defense mechanism that prevents infecting nematode growth and reproduction, and eventually leads to their death (26). Melanotic encapsulation involves both the humoral and cellular components of the innate immune response in mosquitoes. Upon recognition of a pathogen, the cellular arm of insect innate immunity drives aggregation of hemocytes to form a multicellular layer around the invading pathogen. Concurrently, the humoral arm of insect innate immunity initiates melanin production in the hemocytes (27–35). This process is controlled by the phenoloxidase (PO) cascade, which is initiated when a pathogen associated molecular pattern (PAMP) binds to its pattern recognition receptor (PRR) to initiate a serine protease cascade. This cascade ultimately leads to the activation of a pro-phenoloxidase activating factor which in turn will activate phenoloxidase

(26,36,37). Phenoloxidase can then oxidize phenols to quinones which are further polymerized to melanin (38). Death of the parasite is believed to be due to nutrient deprivation, asphyxiation, and/or through the production of toxins such as quinones and other reactive oxygen species produced during melanin production (39,40).

The mechanistic basis for nematode manipulation of mosquito immune responses is not clear but recent studies exploring vector host global transcriptomic changes in response to parasite invasion have identified downregulation of immune-related genes during infection (41–43). A consensus view is that the cumulative effect of this modulation, be it within the intermediate or definitive host, is to suppress the host immune response towards a tolerant state in which the immune response is still present and active, but damage to the parasite is limited. While there is unequivocal evidence that parasites can directly modulate the host immune response, and although the concept is broadly accepted, the parasite-derived effectors that drive this modulation at the cellular and molecular level remain unclear and poorly understood, especially within the context of the vector host.

Parasite excretory-secretory products (ESP) are a well-established source of potential effector molecules. Parasite ESP encompass freely secreted proteins and nucleic acids, as well as extracellular vesicles (EVs), which are membrane-bound structures secreted by both prokaryotic and eukaryotic cells including filarial nematodes (15,44–47). They contain complex cargo that can include proteins, small RNA species, and lipids (48,49) and have been shown to be highly involved in cell-to-cell communication and have roles in various physiological processes (48,50–52). Although EVs are a newly recognized fraction of parasitic nematode ESP, the cargo of some nematode EVs have been profiled, revealing contents to include protein and small RNA species with predicted immunomodulatory properties (15,44,46,53–61). There is strong evidence that

these EVs have direct involvement in immunomodulation of mammalian hosts (4,15,16,44,53,55,56,60,62,63).

We hypothesize that filarial nematode EVs secreted by infective stages of filarial parasites act as effectors to modulate the immune response of the vector host mosquito. To test this hypothesis, we examined the modulatory effects of *B. malayi* microfilariae (mf) EVs on the global transcriptomic profile of *Aedes aegypti* derived Aag2 cells, an established model for mosquito hemocytes due to their characterized immunocompetence (64). We found that nematode EV treatment drove differential expression of host genes, including a serine protease gene. This gene was shown to have direct involvement in the PO pathway as knockdown of the gene lead to a reduction in PO activity *in vitro.* The effect of microfilariae EVs was subsequently investigated *in vivo,* and it was found that these microfilariae derived EVs inhibited PO activity in adult female *A. aegypti*. These findings provide evidence that parasite derived extracellular vesicles contain cargo that are capable of modulating critical vector host immune responses.

2. Results

2.1 *B. malayi* mf derived EVs are internalized by Aag2 cells

To confirm that EVs were being isolated from spent media, EVs were imaged using TEM (Fig. 1A). Particles isolated from spent media exhibited the classic exosome-like deflated soccer ball morphology under EM but such structures were absent from unconditioned media. Vesicle size was further validated with nanoparticle tracking analysis using NanoSight LM10 (Malvern Panalytical, Malvern UK)(Fig. 1B) and showed that the isolated EVs had a mean size and concentration of 92.2 nm and 2.68 x 10^9 particles/ml respectively, well within the expected 50-

200nm range. To investigate the potential for parasitic excretory-secretory products to interact with vector host immune cells, we treated Aag2 cells, an immunocompetent *A. aegypti* cell line (64), with PKH67 stained *B. malayi* mf derived EVs. 24 hours after treatment, cells were additionally stained with DAPI and phalloidin, and imaged with confocal microscopy. Aag2 cells were shown to internalize *B. malayi* mf derived EVs as compared to control cells (Fig. 1C-D). EVs appeared in punctate areas within the cell and were not found diffused throughout the cytoplasm. This correlates with previous evidence that EVs are internalized via endocytosis and thus would be confined to endosomes within the cytoplasm (65). In addition, internalization of parasite EVs by murine epithelial cells showed a similar punctate appearance (15). However, a different phenotype was seen by parasite EVs internalized by murine macrophages and human monocytes where the EVs appeared diffused throughout the cytoplasm (44,46,53). These differences in internalization appearance may be due to various endocytosis pathways utilized by the various cell types. To begin to tease apart the endocytic mechanism by which mf EVs are being internalized, Aag2 cells were treated with the endocytosis inhibitors chlorpromazine (CPZ) and nystatin. CPZ is an inhibitor of clathrin-mediated endocytosis and has been shown to inhibit the function of a key clathrin-mediated endocytic adaptor protein AP2 (66,67). Nystatin is capable of binding cholesterol and thus can inhibit caveolin-mediated endocytosis (68). It was observed that chlorpromazine, but not nystatin inhibited the endocytosis of *B. malayi* mf EVs (Fig. 1E-F), suggesting that the mechanism of endocytosis of parasitic EVs is clathrin-mediated. EV internalization was quantified using flow cytometry (Supplemental Fig. 1). 51% of Aag2 cells internalized *B. malayi* mf EVs as compared to untreated cells ($p < 0.0001$, $N = 3$). Treatment with the endocytosis inhibitor chlorpromazine reduced the number of Aag2 cells that internalized *B. malyi* mf EVs by 39% as compared to EV only treated cells ($p = 0.0003$, $N = 3$).

148 However, the endocytosis inhibitor nystatin did not significantly inhibit EV internalization as
149 compared to EV only treated Aag2 cells.

150

151 **2.2 EV Treatment suppresses miRNA expression with Immune Related Targets**

152 Due to the immunomodulatory cargo identified in other *B. malayi* life stages (44,46), we
153 hypothesized that Aag2 cell phenotypes would be modulated by treatment with *B. malayi* mf
154 EVs. To simulate a naturally occurring infection, Aag2 cells were first treated with LPS
155 (500ng/ml) to mimic the immune response that would initially occur during the early stages of
156 infection. 12 hours later, the cells were then treated with either dPBS or *B. malayi* mf EVs to
157 examine the modulatory effects of EV treatment on an established response. 16 hours later cells
158 were collected and processed for miRNA sequencing. Of the 300 miRNAs identified, 196 were
159 expressed in all three treatment groups (control, LPS only, and LPS + EV). The control treatment
160 group shared 21 miRNAs with the LPS only treatment group and 12 with LPS + EV while LPS
161 and LPS + EV shared 10 common miRNAs. The control, LPS and LPS + EV treatment groups
162 had 40, 19 and two miRNAs that were unique to each treatment group, respectively (Fig 2A). To
163 investigate the ability of *B. malayi* EVs to regulate an immune response, we compared miRNA
164 expression between LPS and LPS + EV treatment groups. Six miRNAs were identified to be
165 significantly downregulated in LPS+EV as compared to LPS only, including aae-mir-1175, aae-
166 mir-2945, bmo-mir-6497, nlo-mir-275, aae-mir-184, and PC-5p-30141_33 (Fig 2B). Target
167 prediction was conducted on these differentially expressed miRNA followed by GO analysis of
168 the predicted gene targets. Targets were identified for five out of the six downregulated miRNAs
169 with gene targets of these downregulated miRNAs having roles in proteolysis, regulation of
170 transcription, signal transduction, phagocytosis, and cell differentiation among others (Fig 2C).

Additionally, KEGG analysis identified that the predicted gene targets are involved in multiple immune related pathways (Table 1). Gene targets of the downregulated miRNAs are predicted to be involved in common insect immune signaling pathways such as Toll/IMD, MAPK, TGFβ and insulin signaling pathways among others. Some of the predicted gene targets include AAEL008634, a jnk protein; AAEL010433, a transcriptional co-repressor, AAEL003505; a jun protein; and AAEL013433, a spaetzle-like cytokine. One of these miRNAs, aae-mir-1175, is conserved in *Anopheles gambiae* and was shown to be downregulated in plasmodium infected mosquitoes as compared to non-infected mosquitoes (69). In addition, mir-1175 has been identified to be solely expressed in the mosquito midgut a critical barrier in parasite development and transmission in the vector host. A similar phenotype was seen in *A. aegypti* where aae-mir-1175 was downregulated in mosquitoes infected with dengue virus as compared to non-infected mosquitoes(70). This provides evidence for a conserved immunomodulation phenotype across diverse vector pathogens that enables pathogen migration and development. *A. aegypti* infected with *Wolbachia* showed a similar downregulation of aae-mir-2945 when compared to non-infected mosquitoes providing additional support for downregulation of miRNAs to drive immunomodulation. The direct role that downregulating these miRNAs have on insect immune cell responses remain unknown, but these data suggest that *B. malayi* EVs are capable of modulating post-transcriptional control of host gene expression, including genes potentially involved in mosquito immune signaling pathways. Additional experimentation needs to be conducted to determine what specific effector molecule in the EV cargo is driving this modulation.

2.3 Microfilariae EVs downregulate predicted immune related genes *in vitro*

mRNA-seq analysis was conducted concurrently with miRNA-seq analysis. Many differentially expressed genes between LPS and LPS + EV treatment groups were identified (Fig. 3A). A majority of the most highly upregulated or downregulated genes were uncharacterized protein coding genes with unknown function. Thus, rather than focusing on these most differentially regulated targets, genes that were significantly differentially expressed but also moderately annotated were instead chosen for *in vitro* validation. For example, AAEL024490 is a predicted cys-loop ligand-gated ion channel (cysLGIC) subunit with high sequence identity to a predicted gamma-aminobutyric acid (GABA) gated chloride ion channel (CLIC) subunit (this subunit will be referred to as a CLIC subunit for simplicity). AAEL002590 is a putative serine protease that has a *Culex quinquefasciatus* ortholog that has been identified as a pro-phenoloxidase activating factor (PPAF). Both the CLIC subunit gene and the serine protease gene were significantly downregulated upon EV treatment by 99% ($p = < 0.0001$) and were among the genes chosen for *in vitro* validation using RT-qPCR. Aag2 cells were stimulated with LPS to elicit an immune response and then followed with treatment of serial dilutions of *B. malayi* mf EVs. The CLIC subunit was significantly downregulated, expression was reduced by 68% when treated with $1x10^5$ EVs ($p = 0.0369$, $N = 3$) (Fig. 3B) as compared to LPS only treated cells. EV treatment suppressed CLIC expression to basal levels observed in non-LPS treated Aag2 cells (53% of LPS stimulated value, $p = 0.0425$, $N = 3$). The serine protease gene was also significantly downregulated after treatment with $1x10^5$ *B. malayi* mf EVs (57%, $p = 0.0223$, $N = 3$) (Fig. 3C). Again, EV treatment completely abrogated the LPS stimulation of expression ($p = 0.0271$, $N = 3$). These findings are biologically relevant as $1x10^5$ EVs is within the range of anticipated EVs that would be present in a mosquito after a blood meal. While the number of mf taken up by a mosquito during a blood meal varies on the microfilariae density in the blood of the host, it has

been established that the approximate mean number of mf taken up by a mosquito is between 1-300 mf with most taking up approximately 40 mf (71–73). In addition, it has been shown that *B. malayi* mf secrete, on average, 4000 EVs per mf in 24 hours (47). These data provide the approximate range of EVs that would be present in a mosquito within 24 hours of a blood meal would be between $1 \times 10^5 - 1 \times 10^6$. Since AAEL002590 was identified as a serine protease with homology to a *C. quinquefasciatus* PPAF, we next wanted to investigate whether this gene was involved in the PO pathway. RNAi was used to knockdown AAEL002590 in Aag2 cells with a time course experiment showing that optimal knockdown occurred at 24 hrs post-RNAi treatment with 79% suppression of AAEL002590 expression ($p = 0.0012$, $N = 3$) (Supplemental Figure 3). To investigate whether AAEL002590 was involved in the PO pathway, Aag2 cells were treated with duplexed siRNA or scrambled siRNA as a negative control for 24 hrs. Following RNAi treatment cells were either treated with dPBS to quantify changes in basal PO activity or challenged with LPS (500ng/ml) for 6 or 24 hours after which cell culture supernatant was collected and mixed with L-DOPA for the PO activity assay. The assay was incubated overnight and basal PO activity was measured at 490nm. Basal PO activity was inhibited by 36% after AAEL002590 RNAi as compared to control cells at 6 hours ($p = 0.0002$, $N = 3$) and inhibited by 54% as compared to control at 24 hours ($p = 0.018$, $N = 3$) (Fig 3D). While LPS treatment has been used to induce an immune response in Aag2 cells previously (64) and was successful in inducing an immune response in Aag2 cells as evident by our gene expression experiments, LPS did not sufficiently induce the PO cascade *in vitro*. However, it is clear from RNAi-mediated knockdown of basal PO activity that AAEL002590, a target for parasite EV modulation, is involved in the host PO pathway.

GO enrichment analysis was conducted on all significantly ($p \leq 0.05$) upregulated or downregulated mRNAs. We found that genes upregulated following EV treatment were enriched for GO terms associated with metabolic processes and oxidoreductase activity (Fig. 4A). Some increases in metabolic activity and increases in oxidoreductase activity can be explained by the vector's reaction to initial parasite infection. However, increases in steroid and lipid biosynthesis may be driven by parasite effector molecules. It has been shown that host steroid hormones can be influenced by development of parasites and dictate their course of infection, with increase production of steroid hormones leading to more rapid development and longer infections (74,75). In addition, it has been shown that host lipid biosynthesis is hijacked by parasites and is a common them in vector-borne diseases(76).

Genes that were downregulated after EV treatment were enriched for GO terms associated with signaling and immune responses (Fig. 4B). Signaling GO terms include ligand-gated ion channel activity, transmembrane ion transporter activity, neurotransmitter release and neurotransmitter secretion. As mentioned previously, we have already validated that a predicted GABA-gated chloride ion channel subunit is downregulated after EV treatment. The GABAergic system has been highly implicated in human immune functions including roles in phagocytosis, cytokine production, and cell proliferation(77). While the main findings in humans have concluded that the GABAergic system leads to immunosuppressive phenotypes, the possible role of GABA receptors in invertebrate immune responses has not been well studied. In insects, the cysLGIC superfamily is known for its inhibitory roles in neurotransmission and as target sites for insecticides(78). Dieldrin and endosulfan are organochlorine-based insecticides that function as GABA receptor antagonists and it has been shown that sub-lethal doses of both dieldrin and

endosulfan inhibited the encapsulation of *Leptopolina boulardi* eggs by *Drosophila* larvae(79). The strong body of evidence that GABA receptors are involved in mammalian neurohormonal immune regulation and that certain GABA receptor antagonists in insects can modulate encapsulation, suggests a potential role for the predicted GABA-gated chloride channel in neurohormonal regulation of mosquito immune responses. In particular, a role in promoting or driving the encapsulation process.

2.4 Phenoloxidase activity is inhibited by EV treatment

Having established that parasite EV treatment modulates AAEL002590 in Aag2 cells *in vitro*, we next wanted to determine if this phenotype was recapitulated *in vivo*. Adult female mosquitoes were injected with LPS (1mg/ml) followed by injection with mf EVs or dPBS 6 hours later. Mosquitoes were incubated for 24 hours and then AAEL002590 expression was assayed by RT-qPCR. Injection with $1x10^5$ mf EVs significantly downregulated the serine protease gene by 84% ($p = 0.02$, $N = 3$) as compared to LPS only (Fig. 5A). This EV-suppression returned AAEL002590 expression to basal levels comparable to control mosquitoes in which AAEL002590 expression was 74% lower than LPS stimulated mosquitoes ($p = 0.05$, $N = 4$). Since we had already shown that knockdown of the serine protease gene in Aag2 cells inhibited PO activity *in vitro* we wanted to investigate if *B. malayi* mf EVs could inhibit PO activity *in vivo*. Adult female mosquitoes were treated as previously described and hemolymph was collected by perfusion following the 24-hour incubation. Hemolymph was then mixed with L-DOPA and PO activity was measured by optical density (OD) readings at 490nm every 5 minutes for 30 minutes and a final reading at 60 minutes. PO activity was significantly inhibited in hemolymph from mosquitoes injected with $1x10^5$ mf EVs at all time points. Specifically, PO activity was inhibited by 65% ($p < 0.05$), 81% ($p < 0.0001$), 80% ($p < 0.0001$), 78% ($p <$

286 0.0001), 76% ($p < 0.0001$), 74% ($p < 0.0001$), 72% ($p < 0.0001$), and 64% ($p < 0.0001$) at 0, 5,
287 10, 15, 20, 25, 30 and 60 minutes respectively (all N = 3) as compared to LPS only treated
288 mosquitoes. These results indicate that *B. malayi* mf EVs inhibit PO activity *in vivo* at
289 biologically relevant concentrations. While the PO activity induced by LPS treatment may not
290 have appeared as high as predicted, the pronounced inhibition after EV treatment is compelling.

291

292 ## 3. Discussion

293 While there is strong evidence for parasite-derived host immunomodulation of the mammalian
294 host, evidence of immunomodulation of the vector host is lacking. Here we have shown that
295 parasite-derived extracellular vesicles (EVs) elicit transcriptional changes in an insect immune
296 cell model, specifically, our data show that *B. malayi* mf derived EVs can modulate multiple
297 genes involved in the humoral immune response. The humoral immune response of a mosquito is
298 comprised of pattern recognition receptors (PRRs), antimicrobial peptides (AMPs) and
299 components of the phenoloxidase (PO) cascade. Downregulation of genes involved in these
300 immune responses would be advantageous for any invading pathogen, especially those that must
301 migrate through the mosquito hemolymph. Melanotic encapsulation is a fundamental mosquito
302 defense mechanism against parasites that involves the PO cascade and here we have identified a
303 serine protease with homology to a known prophenoloxidsae activating factor (PPAF) that is
304 downregulated when mosquito cells are treated with *Brugia* EVs. Independent RNAi-mediated
305 knockdown of this serine protease leads to an inhibition in PO activity in an insect cell line. We
306 were also able to show that this phenotype is recapitulated during *Brugia* infection of mosquitoes
307 *in vivo.* Further experimentation is needed to determine if this serine protease is indeed a true

PPAF or if it is a serine protease involved in an upstream cascade that activates pro-PPAF. In either case, however, our data provides evidence that parasite-derived EVs are effector structures in immunomodulation of vector hosts with the ability to interfere with critical host immune responses (Fig 6). Modulation of the vector host melanization immune response is logical as it is the main vector defense mechanism against large, extracellular pathogens such as parasitic nematodes. While our data provides novel mechanistic evidence for modulation of the host melanization immune response, this phenomenon seems to be central to parasite-vector host interactions. Christensen and LaFond (1986) were the first to provide evidence for parasite-derived modulation of the melanization response, showing that *B. pahangi* infected *A. aegypti* had reduced ability to melanize when challenged with intrathoracic inoculation of new *B. pahangi* mf (25). In addition, targeting of the melanization and encapsulation immune response is a common phenotype seen in infections of *Galleria mellonella* with the parasitic nematode *Steinernema carpocapsae.* Studies have shown that a trypsin-like serine protease secreted by *S. carpocapsae* can inhibit PO activity *in vitro* and affects the morphology of *S. capocapsae* hemocytes and inhibits their ability to spread, a feature necessary for encapsulation (80). Further, a secreted chymotrypsin protease from *S. carpocapsae* has also been shown to inhibit PO activity and encapsulation of *G. mellonella* hemocytes both *in vitro* and *in vivo* (81). *Brugia* are known to actively secrete a number of proteases some of which may be involved in modulating the melanization response; indeed, a cathepsin L-like protease is abundantly found in the EVs of infective third stage larvae isolated from *A. aegypti* (44) that is essential to parasite survival within the mosquito (82). An important next step will be to characterize the cargo of *B. malayi* mf EVs to identify those effector molecules responsible for PO pathway downregulation. As this work continues, it will be essential to consider that the modulatory molecules may not be

proteins. We have shown that filarial nematode EVs also contain a diverse miRNA cargo (44) and secreted EVs represent a way that effector miRNAs can be released from the parasite and protected during trafficking to host cells, where they might downregulate immune pathways at the genetic level.

To this end, several transcriptomic studies have looked at the global transcriptional changes that occur in the mosquito host during parasite infection (41–43,83–85). Many of these studies also identified parasite-derived downregulation of mosquito host serine proteases at the genetic level. A study conducted on *B. malayi*-infected *Armigeres subalbatus* showed that there was a significant reduction in expression of multiple serine protease genes during the first 24 hours of infection (41). This correlates with the time frame that EV-secreting mf would be migrating from the midgut, through the hemocele and to the thoracic musculature, and the timeframe seen in our studies. While *B. malayi* do not effectively develop to infective L3 stage parasites in *A. subalbatus*, it still provides evidence for host transcriptional changes during early stages of infection. Similar trends were observed in *B. malayi* infected *A. aegypti* where there was evidence for parasite derived alteration in expression of genes involved in blood digestion and immune function including specific downregulation of serine protease genes (43), providing broad evidence for parasite immunomodulation in a compatible vector model. In addition, a study looking at transcriptional changes in both *B. malayi* and *A. aegypti* during the course of infection saw that between 2-4 days post infection, the *A. aegypti* serine protease gene, AAEL002590, was downregulated in infected mosquitoes (84). This downregulation occurring 2-4 days post infection correlates with our study as 2 days post infection broadly aligns with the mf to L1 molt within the thoracic muscles but some mf will still be present (43). It is also important to note that while our data shows downregulation occurring as early as 24 hours post

354 treatment, this may be due to the fact that we are injecting isolated EVs and not infecting with
355 live parasites. Many of these transcriptomic studies also identified downregulation of CLIP
356 serine proteases or prophenoloxidase enzymes (43,83,85), key components involved in the
357 prophenoloxidase cascade and melanization immune response, providing additional
358 corroboration for our observation that *B. malayi* mf EVs are interfering with this immune
359 response. While our study provides a mechanism for parasite-derived transcriptional changes of
360 the host, all these transcriptional studies provide a substrate for further studies aimed at better
361 understanding mosquito immune responses. Paying particular attention to those mosquito genes
362 that filarial nematode parasites have been selected to suppress over millions of years of the host-
363 parasite interaction may reveal the most critical pathways and proteins to exploit for insecticides
364 or novel transmission control strategies.

365

366 **Figure 6. *B. malayi* microfilariae release EVs that interfere with the PO cascade and**
367 **melanization**

368 Melanotic encapsulation is a common insect defense mechanism against parasites. Upon
369 recognition of a parasite, hemocytes aggregate forming a multicellular layer that deposits a
370 melanin-enriched capsule around the invading parasite. Melanin production is controlled by the
371 phenoloxidase (PO) cascade, which through a series of interdependent reactions, leads to the
372 activation of PO that oxidizes phenols to quinones, which are further polymerized to melanin.
373 Death of the parasite is believed to be due to nutrient deprivation, asphyxiation, or through the
374 production of toxins such as quinones and other reactive oxygen species produced during
375 melanin production. *B. malayi* microfilariae-derived extracellular vesicles downregulate a serine

protease that functions either at the serine protease cascade or as a PPAF, either way interfering with the production of PO and thus inhibiting melanization of invading parasites.

There is a growing body of evidence that host immunomodulation by parasite-derived EVs is a common motif in parasitic nematode infections. This picture began to emerge with seminal work from Buck et al. (2014) who showed that EVs released by the murine gastrointestinal nematode, *Heligmosomoides polygyrus* suppressed expression of an IL-33 receptor subunit (also known as ST2) in intestinal epithelial cells (15,16). IL-33 is an alarmin cytokine that plays an important role in initiation of type 2 immune responses, is critical for driving induction of Th2-associated cytokines, and is involved in the expulsion of intestinal parasitic nematodes (86). This work was extended to show that the same EVs elicited similar modulatory phenotypes in macrophages (16). Further studies have shown that *Trichinella spiralis* EVs are capable of producing some of the modified type 2 immune response phenotypes seen in chronic infections. *T. spiralis* EVs have been shown to downregulate the pro-inflammatory cytokines IL-1β, TNFα, and IFNγ while also increasing production of the anti-inflammatory cytokines IL-10 and TGF-β in an induced colitis mouse model (4). Similarly, *Nippostrongylus brasiliensis* EVs were able to reduce IL-1β and increase IL-10 expression in a similar induced colitis mouse model (55). Importantly, our group and others have shown that the modulation of host biology via EVs is not limited to gastrointestinal parasitic nematodes but also occurs at the filarial nematode-host interface. We have previously described how EVs released by infective L3 stage *B. malayi* drive a phenotype in murine macrophages that is more consistent with classical activation than alternative activation (44). More compelling, evidence generated by the Nutman laboratory shows that EVs secreted by *B. malayi* mfs inhibit phosphorylation of the mTOR complex in human monocytes

399 and point to these EVs as the critical parasite-derived factor eliciting Dendritic cell dysfunction
400 during filarial disease (53). The data from these various studies collectively show parasite-
401 derived EVs driving diverse but consistent effects in mammalian host, an observation that we
402 now extend to the vector host.

403 Our understanding of the filarial nematode-vector interface is incomplete, but the data described
404 in this paper helps to begin addressing this knowledge gap and may even seed the identification
405 of novel targets that could contribute to better controlling filarial nematode diseases. Identifying
406 targets at the vector stage of parasite development may stop transmission of the causative agents
407 of filarial diseases and may provide insight into control strategies for other non-filarial, vector-
408 borne diseases. Any mechanism that disrupts the vector-parasite interaction and skews the
409 balance in favor of the vector is likely to prevent infection, parasite development and
410 transmission.

411

412 # 4. Materials and Methods

413 ## 4.1 Cell culture

414 The immunocompetent *Aedes aegypti*-derived Aag2 cell line was cultured in Schneider's
415 *Drosophila* medium supplemented with 10% heat-inactivated, fetal bovine serum and 1%
416 Penicillin/Streptomycin (all Thermo Fisher Scientific, Waltham, MA, USA) at 28°C.

417 ## 4.2 Parasite Culture and Maintenance

418 *Brugia malayi* parasites were obtained from the NIH/NIAID Filariasis Research Reagent
419 Resource Center (FR3) at the University of Georgia, USA. Persistent *B. malayi* infections at FR3

are maintained in domestic short-haired cats. Microfilariae stage *B. malayi* were obtained from a lavage of the peritoneal cavity of a euthanized gerbil. Microfilaria were washed according to FR3 protocols upon arrival at Iowa State University. Briefly, microfilariae were centrifuged at 2000 rpm for 10 minutes at room temperature to pellet parasites. Transport media [RPMI with Penicillin (2000 U/ml) and Streptomycin (2000 µg/ml)] was aspirated and the parasite pellet resuspended in dPBS (Thermo Fisher Scientific). The parasite suspension was overlaid onto 10 ml of Histopaque-1077 (Sigma Aldrich, St. Louis, MO, USA) and centrifuged at 2000 rpm for an additional 15 minutes. The supernatant was aspirated and parasite pellet washed with dPBS twice for 5 minutes each wash. After washing, the supernatant was aspirated and 3 ml of cell culture grade water (Cytiva, Marlborough, MA, USA) was added to the remaining pellet to lyse red blood cells (RBCs). Immediately following RBCs lysis, 10 ml dPBS was added and parasites centrifuged for an additional 5 minutes then washed one final time in dPBS. Microfilariae were then resuspended in worm culture media (RPMI with 1% 1 M HEPES, 1% 200mM L-glutamine, Penicillin (2000 U/ml), Streptomycin (2000 µg/ml), and 1% w/v glucose [all Thermo Fisher Scientific]) and cultured at 37°C with 5% CO_2 for 5-7 days. Parasite motility was used as an indicator of parasite viability. Parasite viability was checked daily and spent media was collected every 24 hours and retained for EV isolation as long parasites appeared viable.

4.3 Mosquito Rearing

A. aegypti (Liverpool strain) mosquitoes were reared at 27°C and 80% relative humidity with a 14:10 h light/dark period. Larvae were fed a 50:50 diet of Tetramin ground fish flakes (Tetra, Melle, Germany) and milk bone dog biscuits. Adults were maintained on a 10% sucrose solution. All experimental techniques were performed on cohorts of 4–6 days old adult female mosquitoes.

4.4 EV Isolation, Quantification & Imaging

EVs were isolated from spent culture media via differential ultracentrifugation as previously described (44,46,47). Briefly, media was filtered through 0.2 µm PVDF filtered syringes (GE Healthcare, Chicago, IL, USA) and centrifuged at 120,000 x *g* for 90 minutes at 4°C. The supernatant was decanted leaving approximately 1.5 ml media to ensure that the EV pellet was not disrupted. The retained media and pellet were filtered through a PVDF 0.2 µm syringe filter and centrifuged at 186,000 x *g* for a further 2 h at 4°C. The size profile and concentration of EVs in the isolated sample were quantified using nanoparticle tracking analysis (NTA; NanoSight LM10, Malvern Instruments, Malvern, UK). EV integrity and morphology were confirmed using transmission electron microscopy (TEM). Briefly, a 2 µl aliquot of EV preparation was placed onto a carbon film grid (Electron Microscopy Sciences, Hatfield, PA, USA) for 1 minute. The drop was wicked to a thin film and 2 µl of uranyl acetate (2% w/v final concentration) was immediately applied for 30 seconds, wicked, and allowed to dry. Images were taken using a 200kV JEOL 2100 scanning and transmission electron microscope (Japan Electron Optics Laboratories, LLC, Peabody, MA) with a Gatan OneView camera (Gatan, Inc. Pleasanton, CA).

4.5 EV internalization by Aag2 cells

Methods were based on protocols previously described (46), but modified for optimal imaging of the Aag2 cell line. 3 $x10^5$ Aag2 cells were seeded on an 18 mm, #1 thickness, poly-D-lysine coverslip (Neuvitro, Vancouver, WA) in a 12-well plate (Thermo Fisher Scientific) and cultured at 28°C overnight. Between $5x10^8$-$1x10^9$ isolated EVs were stained with PKH67 (Sigma Aldrich, St. Louis, MO) according to manufacturer's instructions. Confluent Aag2 cells were treated with $3.5x10^7$ stained EVs and incubated for 24 hrs at 28°C. EV uptake was visualized with immunocytochemistry. Media was removed and cells were washed with 1X dPBS and fixed in

4% paraformaldehyde (Electron Microscopy Sciences) for 15 minutes at room temperature. Following three 1X dPBS washes at room temperature, cells were incubated with 1:300 Alexa Fluor 647 phalloidin (Thermo Fisher Scientific) for 45 minutes at room temperature followed by three washes of 1x dPBS for 5 minutes each. Cells were incubated with 300 nM DAPI (Thermo Fisher Scientific) for 5 minutes at room temperature followed by two washes in 1X dPBS. Coverslips were mounted using Flouromount aqueous mounting media (Sigma Aldrich) and visualized by a Leica SP5 X MP confocal/multiphoton microscope system (Leica Microsystems Inc., Buffalo Grove, IL, USA).

Concurrently, EV internalization was quantified using flow cytometry. 3 $x10^5$ cells were seeded per well of a 12-well plate and incubated at 28°C overnight. Cells were incubated with $3.5x10^7$ PKH67 stained EVs for 24 hrs at 28°C. Cells were washed in 1x dPBS and collected into polystyrene FACS tubes (Thermo Fisher Scientific). Cells were fixed in 4% paraformaldehyde for 20 minutes and washed with FACS buffer (dPBS supplemented with 1% BSA and 0.1% NaN_3). Cells were resuspended in 400 µl FACS buffer and analyzed with a BD Accuri C6 Flow Cytometer (BD Biosciences, San Jose, CA). For endocytosis inhibition assays, Aag2 cells were treated with a final concentration of either 30 µM chlorpromazine or 15 µM nystatin (Thermo Fisher Scientific). Following a two-hour incubation, media was changed and cells treated with $3.5x10^7$ *B. malayi* mf EVs, incubated for 24 hours and then collected for confocal microscopy and flow cytometry as described above.

4.6 mRNA-Seq Analysis

1 x 10^5 Aag2 cells were seeded in each well of a 96-well plate (Corning Inc, Corning, NY, USA) and incubated overnight at 28°C. The following day, culture media was changed and cells were treated with either lipopolysaccharide (LPS) (500 ng/ml) to stimulate an immune response *in*

vitro or dPBS as a negative control. Cells were incubated for an additional 12 hours at 28°C after which, culture media was changed and cells treated with 1.1 x 10^9 parasite EVs per well. Cells were then incubated for a further 16 hours at 28°C before collection and storage in Trizol (Thermo Fisher Scientific) ahead of RNA extraction. Briefly, cells in Trizol were mixed with chloroform (0.2 ml chloroform per ml Trizol) and shaken vigorously for 20 seconds. Samples were allowed to sit at room temperature for 3 minutes and then centrifuged at 10,000 x *g* for 18 minutes at 4°C. The aqueous phase was collected, and an equal volume of 100% ethanol was added. RNA was then purified and collected using a RNeasy Mini Kit (Qiagen, Hilden, Germany) according to manufacturer's instructions.

mRNA-seq was performed by LC Sciences (Houston, TX). Total RNA quantity and purity were analyzed using an RNA 6000 Nano LabChip Kit and a Bioanalyzer 2100 (Agilent, Santa Clara, CA). High quality RNA samples with RIN number > 7 were used to construct the sequencing library. mRNA was purified from total RNA (5µg) using Dynabeads Oligo (dT)(Thermo Fisher Scientific) with two rounds of purification. Following purification, mRNA was fragmented into short fragments using a NEB Next Magnesium RNA Fragmentation Module (New England Biolabs, Ipswich, MA, USA) at 94°C for 5-7 minutes. Cleaved RNA fragments were reverse transcribed to cDNA by Superscript II Reverse Transcriptase (Thermo Fisher Scientific) and the resulting cDNA used to generate U-labeled second-stranded DNA using *E. coli* DNA polymerase I, RNase H (both New England Biolabs) and dUTP Solution (Thermo Fisher Scientific). An A-base was added to the blunt ends of each strand, preparing them for ligation to the indexed adapters. Each adapter contained a T-base overhang for ligating the adapter to the A-tailed fragmented DNA. Dual-index adapters were ligated to the fragments, and size selection was performed with AMPureXP beads (Beckman Coulter, Brea, CA, USA). U-labeled second-

stranded DNAs were treated with heat-labile UDG enzyme (New England Biolabs), and ligated products were amplified with PCR by the following conditions: initial denaturation at 95°C for 3 minutes; 8 cycles of denaturation at 98°C for 15 seconds, annealing at 60°C for 15 seconds, and extension at 72°C for 30 seconds; and final extension at 72°C for 5 minutes. The average insert size for the paired-end libraries was 300 bp (±50 bp). Paired-end sequencing was performed on an Illumina Hiseq 4000 (Illumina, San Diego, CA, USA). Reads were adapter and quality trimmed using Trimmomatic (87). HISAT2 (88) and StringTie (89) were used to align surviving reads to the *B. malayi* reference genome (WormBase ParaSite version 12.4) (90,91) and to the *A. aegypti* reference genome (VectorBase release 47) (92) to produce raw counts for annotated genes. The RNA-seq pipeline was implemented using Nextflow (93). DESeq2 (94) and custom R scripts were used to identify differentially expressed genes (DEGs) across conditions. The R package topGO (95) was used to assess functional enrichment of differentially expressed genes. Gene ontology (GO) terms from the *A. aegypti* LVP transcriptome were retrieved from VectorBase (92).

4.7 miRNA-Seq Analysis

microRNA (miRNA) sequencing was performed by LC Sciences. The total RNA quality and quantity were analyzed by Bioanalyzer 2100 (Agilent Technologies, Santa Clara, CA) with RIN number >7.0. Small RNA libraries were prepared using 1 µg of total RNA and the TruSeq Small RNA Sample Prep Kits (Illumina) according to manufacturer's instructions. Single-end sequencing was performed on an Illumina Hiseq 2500 (Illumina) according to manufacturer's instructions. Raw reads were subjected to an in-house program, ACGT101-miR (LC Sciences), to remove adapter dimers and junk, low complexity and common non-target RNA families (rRNA, tRNA, snRNA, snoRNA) and repeats. Remaining unique sequences with length 18~26

nucleotides were mapped to specific species precursors in miRBase 22.0 (96–101) and by BLAST search (102) to identify known miRNAs and novel 3p- and 5p- derived miRNAs with their genomic location. Length variation at both 3' and 5' ends and one mismatch inside of the sequence were allowed in the alignment. The unique sequences mapping to specific species mature miRNAs in hairpin arms were identified as known miRNAs. The unique sequences mapping to the other arm of known specific species precursor hairpin opposite to the annotated mature miRNA-containing arm were considered to be novel 5p- or 3p derived miRNA candidates. Hairpin RNA structures of unmapped sequences were predicted from the flanking 80 nucleotide sequences using RNAfold (103). The criteria for secondary structure prediction included number of nucleotides in one bulge in stem (≤12), number of base pairs in the stem region of the predicted hairpin (≥16), cutoff of free energy (kCal/mol ≤-15), length of hairpin (up and down stems + terminal loop ≥50), length of hairpin loop (≤20), number of nucleotides in one bulge in mature region (≤8), number of biased errors in one bulge in mature region (≤4), number of biased bulges in mature region (≤2), number of errors in mature region (≤7), number of base pairs in the mature region of the predicted hairpin (≥12) and percent of mature sequences in stem (≥80). To predict the genes targeted by most abundant miRNAs, two computational target prediction algorithms TargetScan (104–106) and Miranda 3.3a (107) were used to identify putative miRNA binding sites. Finally, the data predicted by both algorithms were combined and the overlaps calculated. The R package, enrichplot, was used to visualize GO term enrichment from the predicted targets of differentially expressed miRNAs.

4.8 RT-qPCR Validation of Gene Expression Levels

$1x10^5$ Aag2 cells were seeded in each well of a 96-well plate (Corning Inc, Corning, NY, USA) and incubated overnight at 28°C. The following day, culture media was changed and cells were

558 treated with either LPS (500 ng/ml) to stimulate an immune response *in vitro* or dPBS as a
559 negative control. Cells were incubated for an additional 12 hours at 28°C after which, culture
560 media was changed and cells treated with 10-fold serial dilutions ranging from 1 x 10^9 to 1 x 10^2
561 parasite EVs. This range was used as it allowed us to see the effects of treating cells with more
562 EVs than would be present in a natural infection, EV levels present during a natural infection (1
563 x 10^6 – 1 x 10^5) and the effects of having less EVs than would occur in a natural infection. Cells
564 were then incubated for a further 16 hours at 28°C before collection and storage in Trizol
565 (Thermo Fisher Scientific) ahead of RNA extraction described above. cDNA was synthesized
566 from sample RNA using Superscript III First-Strand cDNA Synthesis kit (Thermo Fisher
567 Scientific) according to manufacturer's instructions. 20 ng of cDNA was used per qPCR reaction
568 using Powerup SYBR green master mix (Thermo Fisher Scientific) and gene specific primers
569 according to manufacturer's instructions on a Quantstudio 3 Real-Time PCR system (Thermo
570 Fisher Scientific). CT values were averaged across technical replicates and normalized against
571 RPS17. Primer sequences for AAEL002590 (Serine Protease), AAEL024490 (predicted cys-loop
572 ligand-gated ion channel [cysLGIC] subunit), and the housekeeping gene (RPS17) can be found
573 in Supplemental Table 1**.**

574 **4.9 *In vitro* RNA Interference**

575 Duplexed siRNA was designed and produced targeting the serine protease gene by Integrated
576 DNA Technologies (Coralville, IA, USA). Sequences for the duplexed siRNA can be found in
577 Supplemental Information 3. 4 x 10^4 Aag2 cells were seeded per well of a 96-well plate and
578 incubated overnight. 5 pmol of siRNA or scrambled negative control was mixed with
579 lipofectamine RNAiMAX Reagent (Thermo fisher Scientific) to create a 1 pmol siRNA solution.
580 10 µl of the 1 pmol siRNA solution was added per well and incubated for 24 hours. To determine

RNAi efficiency, total RNA was isolated from cells for subsequent RT-qPCR as described above.

4.10 *Aedes aegypti* Injections

Four to five-day old *A. aegypti* (Liverpool strain) female mosquitoes were intrathoracically injected with 69 nl of LPS (1 mg/ml) [Sigma Aldrich] or dPBS (Thermo Fisher Scientific) using a Nanoject III injector (Drummond Scientific Company, Broomall, PA, USA) and incubated for six hours at 27°C prior to EV injection. Mosquitoes were then challenged with serial dilutions of $1x10^7$, $1x10^6$, $1x10^5$ EVs, or dPBS as a control. Total RNA was isolated from 8 mosquitoes per treatment group 24 hours post-challenge. Mosquitoes were homogenized using a mortar and pestle in 1 ml of Trizol. The resulting suspension was centrifuged at 12,000 x *g* for 10 minutes at 4°C to remove debris, the supernatant collected. RNA extraction, cDNA synthesis and qPCR were performed as previously described.

4.11 Phenoloxidase Activity Assay

Pooled hemolymph was collected from 10 adult female mosquitoes by perfusion and prepared for PO assay as previously described (108). Briefly, 10 µl of hemolymph was mixed with 90 µl of 3, 4-Dihydroxy-L-phenylalanine (L-DOPA, 4 mg/ml)(Sigma Aldrich) dissolved in nuclease free water (Cytiva). After an initial 10 minutes incubation at room temperature, PO activity was measured at 490 nm every 5 minutes for 30 minutes, then the final activity was measured at 60 minutes using a Synergy HTX Multi-Mode Microplate Reader (Agilent). To determine if AAEL002590 was directly involved in the PO pathway AAEL002590 was knockdown via siRNA in Aag2 cells as previously described. After the 24 hr incubation, Aag2 cells were challenged with LPS (500ng/ml) for either 6 or 24 hours. 10 µl of either control or siRNA treated

Aag2 cell culture media was mixed with 90 µl L-DOPA as previously described. PO activity was allowed to proceed at room temperature overnight after which PO activity was measured at 490 nm.

4.12 Statistical Analysis

In vitro RT-qPCR validation was analyzed using a repeated measures one-way ANOVA while *in vivo* RT-qPCR validation was analyzed using mixed effects one-way ANOVA. Multiple comparisons were conducted using the Dunnett statistical hypothesis testing method. Enrichment of functions within the molecular function, biological process, and cellular component GO term sub-ontologies were analyzed using a Fisher's exact test. *In vivo* PO assays were analyzed using a repeated measures two-way ANOVA with a Šidák multiple comparisons test while in vitro PO assays were analyzed with multiple T tests with a Holm- Šidák multiple comparison test. For all significance testing p-values < 0.05 was considered significant. All ANOVAs were completed using GraphPad prism 9.3.1 (GraphPad Software, San Diego, CA, USA).

References

1. World Health Organization. Global programme to eliminate lymphatic filariasis: progress report, 2020 [Internet]. 2021 Oct [cited 2022 Feb 22] p. 12. Available from: https://www.who.int/publications-detail-redirect/who-wer9641-497-508

2. WHO. Lymphatic filariasis [Internet]. World Health Organization. [cited 2022 Jan 20]. Available from: https://www.who.int/news-room/fact-sheets/detail/lymphatic-filariasis

3. Castillo JC, Reynolds SE, Eleftherianos I. Insect immune responses to nematode parasites. Trends in Parasitology. 2011 Dec 1;27(12):537–47.

4. Yang Y, Liu L, Liu X, Zhang Y, Shi H, Jia W, et al. Extracellular Vesicles Derived From Trichinella spiralis Muscle Larvae Ameliorate TNBS-Induced Colitis in Mice. Frontiers in Immunology [Internet]. 2020 [cited 2022 Jan 24];11. Available from: https://www.frontiersin.org/article/10.3389/fimmu.2020.01174

5. Finlay CM, Walsh KP, Mills KHG. Induction of regulatory cells by helminth parasites: exploitation for the treatment of inflammatory diseases. Immunological Reviews. 2014;259(1):206–30.

6. Taylor MD, LeGoff L, Harris A, Malone E, Allen JE, Maizels RM. Removal of Regulatory T Cell Activity Reverses Hyporesponsiveness and Leads to Filarial Parasite Clearance In Vivo. The Journal of Immunology. 2005 Apr 15;174(8):4924–33.

7. Taylor MD, van der Werf N, Harris A, Graham AL, Bain O, Allen JE, et al. Early recruitment of natural CD4+Foxp3+ Treg cells by infective larvae determines the outcome of filarial infection. European Journal of Immunology. 2009;39(1):192–206.

8. KORTEN S, HOERAUF A, KAIFI JT, BÜTTNER DW. Low levels of transforming growth factor-beta (TGF-beta) and reduced suppression of Th2-mediated inflammation in hyperreactive human onchocerciasis. Parasitology. 2011 Jan;138(1):35–45.

9. D'Elia R, Behnke JM, Bradley JE, Else KJ. REGULATORY T CELLS. J Immunol. 2009 Feb 15;182(4):2340–8.

10. Grainger JR, Smith KA, Hewitson JP, McSorley HJ, Harcus Y, Filbey KJ, et al. Helminth secretions induce de novo T cell Foxp3 expression and regulatory function through the TGF-β pathway. Journal of Experimental Medicine. 2010 Sep 27;207(11):2331–41.

11. Harnett W, Harnett MM. Lymphocyte hyporesponsiveness during filarial nematode infection. Parasite Immunology. 2008;30(9):447–53.

12. Hartmann S, Kyewski B, Sonnenburg B, Lucius R. A filarial cysteine protease inhibitor down-regulates T cell proliferation and enhances interleukin-10 production. European Journal of Immunology. 1997;27(9):2253–60.

13. Jenson JS, O'Connor R, Osborne J, Devaney E. Infection with Brugia microfilariae induces apoptosis of CD4+ T lymphocytes: a mechanism of immune unresponsiveness in filariasis. European Journal of Immunology. 2002;32(3):858–67.

14. Mishra R, Panda SK, Sahoo PK, Bal MS, Satapathy AK. Increased Fas ligand expression of peripheral B-1 cells correlated with CD4+ T-cell apoptosis in filarial-infected patients. Parasite Immunology. 2017;39(4):e12421.

15. Buck AH, Coakley G, Simbari F, McSorley HJ, Quintana JF, Le Bihan T, et al. Exosomes secreted by nematode parasites transfer small RNAs to mammalian cells and modulate innate immunity. Nature Communications. 2014 Nov 25;5(1):5488.

16. Coakley G, McCaskill JL, Borger JG, Simbari F, Robertson E, Millar M, et al. Extracellular Vesicles from a Helminth Parasite Suppress Macrophage Activation and Constitute an Effective Vaccine for Protective Immunity. Cell Reports. 2017 May 23;19(8):1545–57.

17. Semnani RT, Venugopal PG, Leifer CA, Mostböck S, Sabzevari H, Nutman TB. Inhibition of TLR3 and TLR4 function and expression in human dendritic cells by helminth parasites. Blood. 2008 Aug 15;112(4):1290–8.

18. Babu S, Bhat SQ, Kumar NP, Lipira AB, Kumar S, Karthik C, et al. Filarial Lymphedema Is Characterized by Antigen-Specific Th1 and Th17 Proinflammatory Responses and a Lack of Regulatory T Cells. PLOS Neglected Tropical Diseases. 2009 Apr 21;3(4):e420.

19. Melendez AJ, Harnett MM, Pushparaj PN, Wong WSF, Tay HK, McSharry CP, et al. Inhibition of Fc epsilon RI-mediated mast cell responses by ES-62, a product of parasitic filarial nematodes. Nat Med. 2007 Nov 1;13(11):1375–81.

20. Ottow MK, Klaver EJ, van der Pouw Kraan TCTM, Heijnen PD, Laan LC, Kringel H, et al. The helminth Trichuris suis suppresses TLR4-induced inflammatory responses in human macrophages. Genes Immun. 2014 Oct;15(7):477–86.

21. Pineda MA, McGrath MA, Smith PC, Al-Riyami L, Rzepecka J, Gracie JA, et al. The parasitic helminth product ES-62 suppresses pathogenesis in collagen-induced arthritis by targeting the interleukin-17–producing cellular network at multiple sites. Arthritis & Rheumatism. 2012;64(10):3168–78.

22. King CL, Mahanty S, Kumaraswami V, Abrams JS, Regunathan J, Jayaraman K, et al. Cytokine control of parasite-specific anergy in human lymphatic filariasis. Preferential induction of a regulatory T helper type 2 lymphocyte subset. J Clin Invest. 1993 Oct;92(4):1667–73.

23. Nutman TB, Kumaraswami V. Regulation of the immune response in lymphatic filariasis: perspectives on acute and chronic infection with Wuchereria bancrofti in South India. Parasite Immunology. 2001;23(7):389–99.

24. Mangan NE, Fallon RE, Smith P, Rooijen N van, McKenzie AN, Fallon PG. Helminth Infection Protects Mice from Anaphylaxis via IL-10-Producing B Cells. The Journal of Immunology. 2004 Nov 15;173(10):6346–56.

25. Christensen BM, LaFond MM. Parasite-Induced Suppression of the Immune Response in Aedes aegypti by Brugia pahangi. The Journal of Parasitology. 1986;72(2):216–9.

26. González-Santoyo I, Córdoba-Aguilar A. Phenoloxidase: a key component of the insect immune system. Entomologia Experimentalis et Applicata. 2012;142(1):1–16.

27. Andreadis TG, Hall DW. Neoaplectana carpocapsae: Encapsulation in Aedes aegypti and changes in host hemocytes and hemolymph proteins. Experimental Parasitology. 1976 Apr 1;39(2):252–61.

28. Drif L, Brehélin M. The circulating hemocytes of Culexpipiens and Aedesaegypii: Cytology histochemistry, hemograms and functions. Developmental & Comparative Immunology. 1983 Sep 1;7(4):687–90.

29. Beerntsen BT, Luckhart S, Christensen BM. Brugia malayi and Brugia pahangi: Inherent Difference in Immune Activation in the Mosquitoes Armigeres subalbatus and Aedes aegypti. The Journal of Parasitology. 1989;75(1):76–81.

30. Beerntsen BT, Severson DW, Christensen BM. Aedes aegypti: Characterization of a Hemolymph Polypeptide Expressed during Melanotic Encapsulation of Filarial Worms. Experimental Parasitology. 1994 Nov 1;79(3):312–21.

31. Paskewitz S, Riehle MA. Response of Plasmodium refractory and susceptible strains of Anopheles gambiae to inoculated Sephadex beads. Developmental & Comparative Immunology. 1994 Sep 1;18(5):369–75.

32. Cupp MS, Chen Y, Cupp EW. Cellular Hemolymph Response of Simulium vittatum (Diptera: Simuliidae) to Intrathoracic Injection of Onchocerca lienalis (Filarioidea: Onchocercidae) Microfilariae. Journal of Medical Entomology. 1997 Jan 1;34(1):56–63.

33. Gorman MJ, Paskewitz SM. A Genetic Study of a Melanization Response to Sephadex Beads in Plasmodium-Refractory and -Susceptible Strains of Anopheles gambiae. The American Journal of Tropical Medicine and Hygiene. 1997 Apr 1;56(4):446–51.

34. Chen CC, Laurence BR. An ultrastructural study on the encapsulation of microfilariae of Brugia pahangi in the haemocoel of Anopheles quadrimaculatus. International Journal for Parasitology. 1985 Aug 1;15(4):421–8.

35. Chikilian ML, Bradley TJ, Nayar JK, Knight JW. Ultrastructural comparison of extracellular and intracellular encapsulation of Brugia malayi in Anopheles quadrimaculatus. J Parasitol. 1994 Feb;80(1):133–40.

36. Cerenius L, Söderhäll K. The prophenoloxidase-activating system in invertebrates. Immunological Reviews. 2004;198(1):116–26.

37. Nakhleh J, El Moussawi L, Osta MA. Chapter Three - The Melanization Response in Insect Immunity. In: Ligoxygakis P, editor. Advances in Insect Physiology [Internet]. Academic Press; 2017 [cited 2022 Jan 20]. p. 83–109. (Insect Immunity; vol. 52). Available from: https://www.sciencedirect.com/science/article/pii/S0065280616300467

38. Nappi AJ, Vass E. Melanogenesis and the Generation of Cytotoxic Molecules During Insect Cellular Immune Reactions. Pigment Cell Research. 1993;6(3):117–26.

39. Kumar A, Srivastava P, Sirisena P, Dubey SK, Kumar R, Shrinet J, et al. Mosquito Innate Immunity. Insects [Internet]. 2018 Aug 8 [cited 2021 Jan 20];9(3). Available from: https://www.ncbi.nlm.nih.gov/pmc/articles/PMC6165528/

40. Lavine MD, Strand MR. Insect hemocytes and their role in immunity. Insect Biochemistry and Molecular Biology. 2002 Oct 1;32(10):1295–309.

41. Aliota MT, Fuchs JF, Mayhew GF, Chen C-C, Christensen BM. Mosquito transcriptome changes and filarial worm resistance in Armigeres subalbatus. BMC Genomics. 2007 Dec 18;8:463.

42. Bartholomay LC, Waterhouse RM, Mayhew GF, Campbell CL, Michel K, Zou Z, et al. Pathogenomics of Culex quinquefasciatus and meta-analysis of infection responses to diverse pathogens. Science. 2010 Oct 1;330(6000):88–90.

43. Erickson SM, Xi Z, Mayhew GF, Ramirez JL, Aliota MT, Christensen BM, et al. Mosquito Infection Responses to Developing Filarial Worms. PLOS Neglected Tropical Diseases. 2009 Oct 13;3(10):e529.

44. Zamanian M, Fraser LM, Agbedanu PN, Harischandra H, Moorhead AR, Day TA, et al. Release of Small RNA-containing Exosome-like Vesicles from the Human Filarial Parasite Brugia malayi. PLoS Negl Trop Dis [Internet]. 2015 Sep 24 [cited 2020 Mar 30];9(9). Available from: https://www.ncbi.nlm.nih.gov/pmc/articles/PMC4581865/

45. Tritten L, Clarke D, Timmins S, McTier T, Geary TG. Dirofilaria immitis exhibits sex- and stage-specific differences in excretory/secretory miRNA and protein profiles. Veterinary Parasitology. 2016 Dec 15;232:1–7.

46. Harischandra H, Yuan W, Loghry HJ, Zamanian M, Kimber MJ. Profiling extracellular vesicle release by the filarial nematode Brugia malayi reveals sex-specific differences in cargo and a sensitivity to ivermectin. PLOS Neglected Tropical Diseases. 2018 Apr 16;12(4):e0006438.

47. Loghry HJ, Yuan W, Zamanian M, Wheeler NJ, Day TA, Kimber MJ. Ivermectin inhibits extracellular vesicle secretion from parasitic nematodes. Journal of Extracellular Vesicles. 2020;10(2):e12036.

48. Thery C, Zitvogel L, Amigorena S. Exosomes: composition, biogenesis and function. Nature Reviews Immunology. 2002 Aug;2(8):569-.

49. Valadi H, Ekstrom K, Bossios A, Sjostrand M, Lee JJ, Lotvall JO. Exosome-mediated transfer of mRNAs and microRNAs is a novel mechanism of genetic exchange between cells. Nature Cell Biology. 2007 Jun;9(6):654-.

50. Bobrie A, Colombo M, Raposo G, Théry C. Exosome Secretion: Molecular Mechanisms and Roles in Immune Responses. Traffic. 2011;12(12):1659–68.

51. Raposo G, Nijman HW, Stoorvogel W, Liejendekker R, Harding CV, Melief CJ, et al. B lymphocytes secrete antigen-presenting vesicles. J Exp Med. 1996 Mar 1;183(3):1161–72.

52. Vlassov AV, Magdaleno S, Setterquist R, Conrad R. Exosomes: Current knowledge of their composition, biological functions, and diagnostic and therapeutic potentials. Biochimica et Biophysica Acta (BBA) - General Subjects. 2012 Jul 1;1820(7):940–8.

53. Ricciardi A, Bennuru S, Tariq S, Kaur S, Wu W, Elkahloun AG, et al. Extracellular vesicles released from the filarial parasite Brugia malayi downregulate the host mTOR pathway. PLOS Neglected Tropical Diseases. 2021 Jan 7;15(1):e0008884.

54. Gu HY, Marks ND, Winter AD, Weir W, Tzelos T, McNeilly TN, et al. Conservation of a microRNA cluster in parasitic nematodes and profiling of miRNAs in excretory-secretory products and microvesicles of Haemonchus contortus. PLOS Neglected Tropical Diseases. 2017 Nov 16;11(11):e0006056.

55. Eichenberger RM, Ryan S, Jones L, Buitrago G, Polster R, Montes de Oca M, et al. Hookworm Secreted Extracellular Vesicles Interact With Host Cells and Prevent Inducible Colitis in Mice. Front Immunol [Internet]. 2018 [cited 2020 Jun 3];9. Available from: https://www.frontiersin.org/articles/10.3389/fimmu.2018.00850/full

56. Eichenberger RM, Talukder MH, Field MA, Wangchuk P, Giacomin P, Loukas A, et al. Characterization of Trichuris muris secreted proteins and extracellular vesicles provides new

insights into host–parasite communication. Journal of Extracellular Vesicles. 2018 Dec 1;7(1):1428004.

57. Tzelos T, Matthews JB, Buck AH, Simbari F, Frew D, Inglis NF, et al. A preliminary proteomic characterisation of extracellular vesicles released by the ovine parasitic nematode, Teladorsagia circumcincta. Veterinary Parasitology. 2016 May 15;221:84–92.

58. Hansen EP, Fromm B, Andersen SD, Marcilla A, Andersen KL, Borup A, et al. Exploration of extracellular vesicles from Ascaris suum provides evidence of parasite–host cross talk. Journal of Extracellular Vesicles. 2019 Dec 1;8(1):1578116.

59. Tritten L, Tam M, Vargas M, Jardim A, Stevenson MM, Keiser J, et al. Excretory/secretory products from the gastrointestinal nematode Trichuris muris. Experimental Parasitology. 2017 Jul 1;178:30–6.

60. Shears RK, Bancroft AJ, Hughes GW, Grencis RK, Thornton DJ. Extracellular vesicles induce protective immunity against Trichuris muris. Parasite Immunology. 2018;40(7):e12536.

61. Hansen EP, Kringel H, Williams AR, Nejsum P. SECRETION OF RNA-CONTAINING EXTRACELLULAR VESICLES BY THE PORCINE WHIPWORM, TRICHURIS SUIS. The Journal of Parasitology. 2015;101(3):336–40.

62. Kosanović M, Cvetković J, Gruden-Movsesijan A, Vasilev S, Svetlana M, Ilić N, et al. Trichinella spiralis muscle larvae release extracellular vesicles with immunomodulatory properties. Parasite Immunology. 2019;41(10):e12665.

63. Duque-Correa MA, Schreiber F, Rodgers FH, Goulding D, Forrest S, White R, et al. Development of caecaloids to study host–pathogen interactions: new insights into immunoregulatory functions of Trichuris muris extracellular vesicles in the caecum. International Journal for Parasitology. 2020 Aug 1;50(9):707–18.

64. Barletta ABF, Silva MCLN, Sorgine MHF. Validation of Aedes aegypti Aag-2 cells as a model for insect immune studies. Parasites & Vectors. 2012 Jul 24;5(1):148.

65. Joshi BS, de Beer MA, Giepmans BNG, Zuhorn IS. Endocytosis of Extracellular Vesicles and Release of Their Cargo from Endosomes. ACS Nano. 2020 Apr 28;14(4):4444–55.

66. Wang LH, Rothberg KG, Anderson RG. Mis-assembly of clathrin lattices on endosomes reveals a regulatory switch for coated pit formation. Journal of Cell Biology. 1993 Dec 1;123(5):1107–17.

67. Vercauteren D, Vandenbroucke RE, Jones AT, Rejman J, Demeester J, De Smedt SC, et al. The Use of Inhibitors to Study Endocytic Pathways of Gene Carriers: Optimization and Pitfalls. Molecular Therapy. 2010 Mar 1;18(3):561–9.

68. Payne CK, Jones SA, Chen C, Zhuang X. Internalization and Trafficking of Cell Surface Proteoglycans and Proteoglycan-Binding Ligands. Traffic. 2007;8(4):389–401.

69. Winter F, Edaye S, Hüttenhofer A, Brunel C. Anopheles gambiae miRNAs as actors of defence reaction against Plasmodium invasion. Nucleic Acids Research. 2007 Nov 1;35(20):6953–62.

70. Campbell CL, Harrison T, Hess AM, Ebel GD. MicroRNA levels are modulated in Aedes aegypti after exposure to Dengue-2. Insect Molecular Biology. 2014;23(1):132–9.

71. Dedkhad W, Christensen BM, Bartholomay LC, Joshi D, Hempolchom C, Saeung A. Immune responses of Aedes togoi, Anopheles paraliae and Anopheles lesteri against nocturnally subperiodic Brugia malayi microfilariae during migration from the midgut to the site of development. Parasites Vectors. 2018 Dec;11(1):1–15.

72. Ramachandran CP. Biological Aspects in the Transmission of Brugia Malayi by Aedes Aegypti in the Laboratory1. Journal of Medical Entomology. 1966 Dec 1;3(3–4):239–52.

73. Albuquerque CM, Cavalcanti VM, Melo MAV, Verçosa P, Regis LN, Hurd H. Bloodmeal microfilariae density and the uptake and establishment of Wuchereria bancrofti infections in Culex quinquefasciatus and Aedes aegypti. Mem Inst Oswaldo Cruz. 1999 Sep;94:591–6.

74. Childs LM, Cai FY, Kakani EG, Mitchell SN, Paton D, Gabrieli P, et al. Disrupting Mosquito Reproduction and Parasite Development for Malaria Control. PLOS Pathogens. 2016 Dec 15;12(12):e1006060.

75. Werling K, Shaw WR, Itoe MA, Westervelt KA, Marcenac P, Paton DG, et al. Steroid Hormone Function Controls Non-competitive Plasmodium Development in Anopheles. Cell. 2019 Apr 4;177(2):315-325.e14.

76. O'Neal AJ, Butler LR, Rolandelli A, Gilk SD, Pedra JH. Lipid hijacking: A unifying theme in vector-borne diseases. Soldati-Favre D, editor. eLife. 2020 Oct 29;9:e61675.

77. Jin Z, Mendu SK, Birnir B. GABA is an effective immunomodulatory molecule. Amino Acids. 2013 Jul;45(1):87–94.

78. Jones AK, Bera AN, Lees K, Sattelle DB. The cys-loop ligand-gated ion channel gene superfamily of the parasitoid wasp, Nasonia vitripennis. Heredity (Edinb). 2010 Mar;104(3):247–59.

79. Delpuech J-M, Frey F, Carton Y. Action of insecticides on the cellular immune reaction of Drosophila melanogaster against the parasitoid Leptopilina boulardi. Environmental Toxicology and Chemistry. 1996;15(12):2267–71.

80. Balasubramanian N, Toubarro D, Simões N. Biochemical study and in vitro insect immune suppression by a trypsin-like secreted protease from the nematode Steinernema carpocapsae. Parasite Immunology. 2010;32(3):165–75.

81. Balasubramanian N, Hao Y-J, Toubarro D, Nascimento G, Simões N. Purification, biochemical and molecular analysis of a chymotrypsin protease with prophenoloxidase suppression activity from the entomopathogenic nematode Steinernema carpocapsae. International Journal for Parasitology. 2009 Jul 15;39(9):975–84.

82. Song C, Gallup JM, Day TA, Bartholomay LC, Kimber MJ. Development of an In Vivo RNAi Protocol to Investigate Gene Function in the Filarial Nematode, Brugia malayi. PLOS Pathogens. 2010 Dec 23;6(12):e1001239.

83. Mayhew GF, Bartholomay LC, Kou H-Y, Rocheleau TA, Fuchs JF, Aliota MT, et al. Construction and characterization of an expressed sequenced tag library for the mosquito vector Armigeres subalbatus. BMC Genomics. 2007 Dec 18;8(1):462.

84. Choi Y-J, Aliota MT, Mayhew GF, Erickson SM, Christensen BM. Dual RNA-seq of Parasite and Host Reveals Gene Expression Dynamics during Filarial Worm–Mosquito Interactions. PLOS Neglected Tropical Diseases. 2014 May 22;8(5):e2905.

85. Juneja P, Ariani CV, Ho YS, Akorli J, Palmer WJ, Pain A, et al. Exome and Transcriptome Sequencing of Aedes aegypti Identifies a Locus That Confers Resistance to Brugia malayi and Alters the Immune Response. PLOS Pathogens. 2015 Mar 27;11(3):e1004765.

86. Humphreys NE, Xu D, Hepworth MR, Liew FY, Grencis RK. IL-33, a Potent Inducer of Adaptive Immunity to Intestinal Nematodes. The Journal of Immunology. 2008 Feb 15;180(4):2443–9.

87. Bolger AM, Lohse M, Usadel B. Trimmomatic: a flexible trimmer for Illumina sequence data. Bioinformatics. 2014 Aug 1;30(15):2114–20.

88. Kim D, Paggi JM, Park C, Bennett C, Salzberg SL. Graph-based genome alignment and genotyping with HISAT2 and HISAT-genotype. Nat Biotechnol. 2019 Aug;37(8):907–15.

89. Pertea M, Pertea GM, Antonescu CM, Chang T-C, Mendell JT, Salzberg SL. StringTie enables improved reconstruction of a transcriptome from RNA-seq reads. Nat Biotechnol. 2015 Mar;33(3):290–5.

90. Howe KL, Bolt BJ, Shafie M, Kersey P, Berriman M. WormBase ParaSite − a comprehensive resource for helminth genomics. Molecular and Biochemical Parasitology. 2017 Jul 1;215:2–10.

91. Howe KL, Bolt BJ, Cain S, Chan J, Chen WJ, Davis P, et al. WormBase 2016: expanding to enable helminth genomic research. Nucleic Acids Research. 2016 Jan 4;44(D1):D774–80.

92. Giraldo-Calderón GI, Emrich SJ, MacCallum RM, Maslen G, Dialynas E, Topalis P, et al. VectorBase: an updated bioinformatics resource for invertebrate vectors and other organisms related with human diseases. Nucleic Acids Res. 2015 Jan 28;43(Database issue):D707–13.

93. Di Tommaso P, Chatzou M, Floden EW, Barja PP, Palumbo E, Notredame C. Nextflow enables reproducible computational workflows. Nat Biotechnol. 2017 Apr;35(4):316–9.

94. Love MI, Huber W, Anders S. Moderated estimation of fold change and dispersion for RNA-seq data with DESeq2. Genome Biology. 2014 Dec 5;15(12):550.

95. Alexa A, Rahnenfuhrer J. topGO: Enrichment Analysis for Gene Ontology. R Package; 2021.

96. Kozomara A, Griffiths-Jones S. miRBase: annotating high confidence microRNAs using deep sequencing data. Nucleic Acids Research. 2014 Jan 1;42(D1):D68–73.

97. Kozomara A, Griffiths-Jones S. miRBase: integrating microRNA annotation and deep-sequencing data. Nucleic Acids Research. 2011 Jan 1;39(suppl_1):D152–7.

880 98. Kozomara A, Birgaoanu M, Griffiths-Jones S. miRBase: from microRNA sequences to function.
881 Nucleic Acids Research. 2019 Jan 8;47(D1):D155–62.

882 99. Griffiths-Jones S, Saini HK, van Dongen S, Enright AJ. miRBase: tools for microRNA genomics.
883 Nucleic Acids Research. 2008 Jan 1;36(suppl_1):D154–8.

884 100. Griffiths-Jones S, Grocock RJ, van Dongen S, Bateman A, Enright AJ. miRBase: microRNA sequences,
885 targets and gene nomenclature. Nucleic Acids Research. 2006 Jan 1;34(suppl_1):D140–4.

886 101. Griffiths-Jones S. The microRNA Registry. Nucleic Acids Research. 2004 Jan 1;32(suppl_1):D109–11.

887 102. Camacho C, Coulouris G, Avagyan V, Ma N, Papadopoulos J, Bealer K, et al. BLAST+: architecture
888 and applications. BMC Bioinformatics. 2009 Dec 15;10(1):421.

889 103. Lorenz R, Bernhart SH, Höner zu Siederdissen C, Tafer H, Flamm C, Stadler PF, et al. ViennaRNA
890 Package 2.0. Algorithms for Molecular Biology. 2011 Nov 24;6(1):26.

891 104. Calvin H. Jan RCF. Formation, Regulation and Evolution of Caenorhabditis elegans 3'UTRs. Nature.
892 2011 Jan 6;469(7328):97.

893 105. Nam J-W, Rissland OS, Koppstein D, Abreu-Goodger C, Jan CH, Agarwal V, et al. Global analyses of
894 the effect of different cellular contexts on microRNA targeting. Mol Cell. 2014 Mar 20;53(6):1031–
895 43.

896 106. Lewis BP, Burge CB, Bartel DP. Conserved Seed Pairing, Often Flanked by Adenosines, Indicates
897 that Thousands of Human Genes are MicroRNA Targets. Cell. 2005 Jan 14;120(1):15–20.

898 107. Enright AJ, John B, Gaul U, Tuschl T, Sander C, Marks DS. MicroRNA targets in Drosophila. Genome
899 Biology. 2003 Dec 12;5(1):R1.

900 108. Kwon H, Hall DR, Smith RC. Prostaglandin E2 Signaling Mediates Oenocytoid Immune Cell Function
901 and Lysis, Limiting Bacteria and Plasmodium Oocyst Survival in Anopheles gambiae. Frontiers in
902 Immunology. 2021;12:3303.

903

904

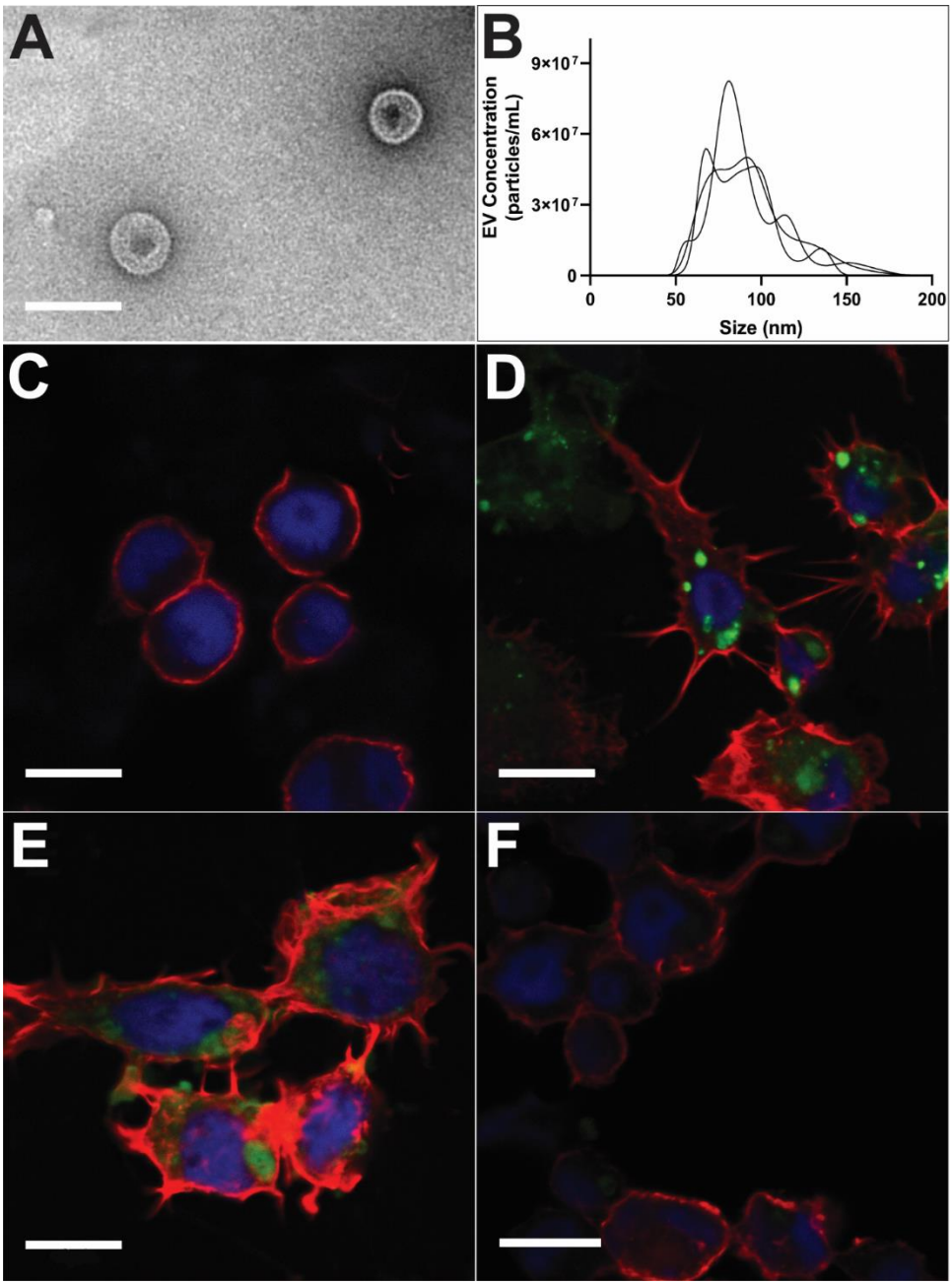

Figure 1. *B. malayi* mf derived EVs are internalized by Aag2 cells

Isolation of *B. malayi* mf EVs was confirmed by TEM (A) and size profile was further validated with nanoparticle tracking analysis (B). PKH67 stained *B. malayi* mf EVs were incubated with Aag2 cells for 24 hours. Cells were stained with Alexa Fluor 647 Phalloidin and DAPI and imaged with a Leica SP5 X MP confocal/multiphoton microscope system. 51% of cells incubated with PKH67 stained EVs showed internalization indicated by the green fluorescence inside the cell (D) as compared to control cells (C). Cells treated with endocytosis inhibitors chlorpromazine (E) showed no endocytosis of stained EVs while cells treated with nystatin (F) showed diffuse uptake of EVs throughout the cytoplasm. Scale bar (A) = 150 nm. Scale bar (C-F) = 10 µM.

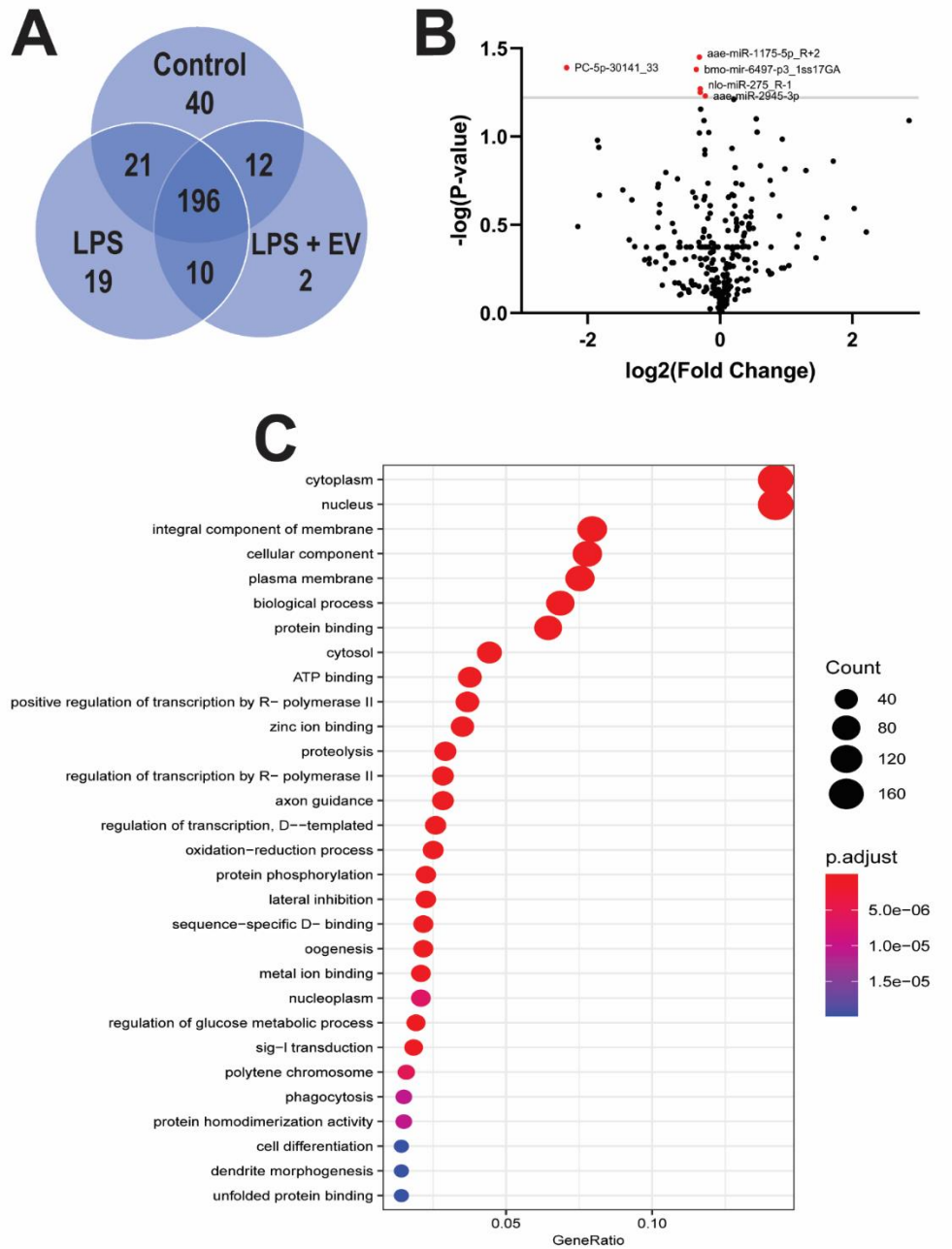

937

938 **Figure 2. EV Treatment suppresses miRNA expression with Immune Related Targets**

939 miRNA-seq analysis was performed on control, LPS and LPS + EV treated Aag2 cells. All three
940 treatment groups shared 196 miRNAs while 40, 19 and two miRNAs were unique to control,
941 LPS only and LPS + EV treatment groups respectively (A). Six significantly, differentially
942 expressed miRNAs were identified between the LPS and LPS + EV treatment groups (B).
943 Predicted targets were identified for five out of the six significantly downregulated miRNAs.
944 Gene ontology (GO) analysis of these predicted gene targets identified their role in various
945 physiological processes including proteolysis, signal transduction and regulation of transcription
946 (C).

miRNA	Function of Predicted Target
aae-mir-1175	MAPK Signaling Pathway
	Longevity Regulating Pathway
	Phosatidylinositol Signaling Pathway
	NOD-like Receptor Signaling Pathway
	Wnt Signaling Pathway
	Notch Signaling Pathway
	TGFβ Signaling Pathway
	FoxO Signaling Pathway
	Toll and Imd Signaling Pathway
aae-mir-2945	Phosatidylinositol Signaling Pathway
	MAPK Signaling Pathway
	Wnt Signaling Pathway
	Toll and Imd Signaling Pathway
	Insulin Signaling Pathway
	Neurotrophin Signaling Pathway
	TGFβ Signaling Pathway
	FoxO Signaling Pathway
	Phosatidylinositol Signaling Pathway
	mTOR Signaling Pathway
	Longevity Regulating Pathway
	Ras Signaling Pathway
bmo-mir-6497	Toll and Imd Signaling Pathway
	MAPK Signaling Pathway
	Notch Signaling Pathway
	Longevity Regulating Pathway
	mTOR Signaling Pathway
	Wnt Signaling Pathway
	FoxO Signaling Pathway
	p53 Signaling Pathway
	Hedgehog Signaling Pathway
	Rap1 Signaling Pathway
	Insulin Signaling Pathway
	Neurotrophin Signaling Pathway
PC-5p-30141_33	Hedgehog Signaling Pathway
	MAPK Signaling Pathway
	TGFβ Signaling Pathway
	mTOR Signaling Pathway

Table 1. KEGG Analysis of downregulated miRNA predicted targets

KEGG analysis of the predicted target genes of the significantly, downregulated miRNAs revealed an enrichment of immune signaling pathways, including common insect immune signaling pathways such as Toll/IMD, MAPK, TGFβ and insulin signaling.

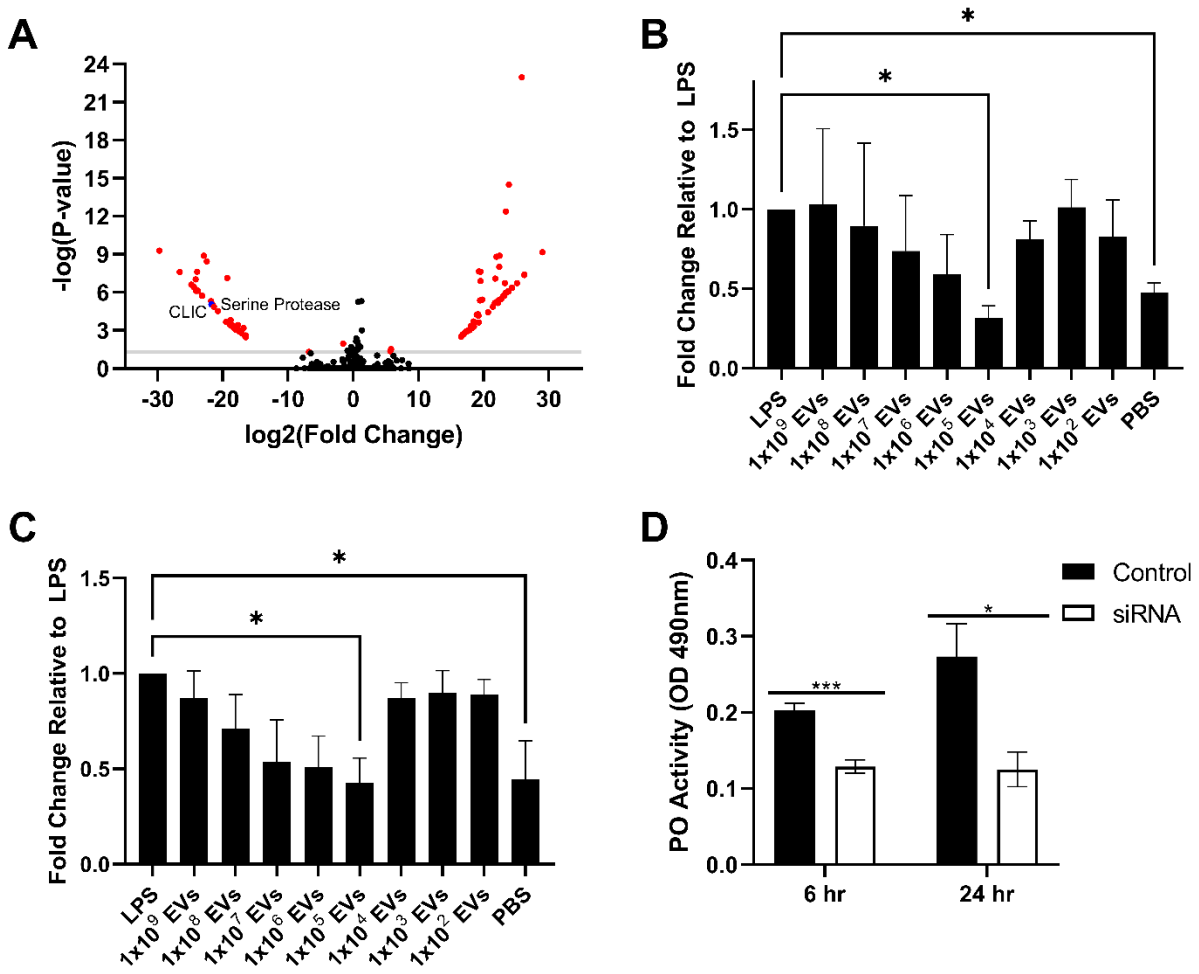

954 **Figure 3. EVs released by *B. malayi* microfilariae downregulate predicted immune related**
955 **genes *in vitro***

956 Multiple genes were differentially expressed between LPS and LPS + EV treatment groups (A).
957 Two moderately annotated and significantly downregulated genes were chosen for further *in*
958 *vitro* validation by RT-qPCR. Both the CLIC subunit gene (B) and the serine protease gene (C)
959 were significantly downregulated when treated with $1x10^5$ *B. malayi* mf EVs as compared to
960 control. RNAi knockdown of the serine protease gene in Aag2 cells inhibited phenoloxidase
961 activity as compared to control at both 6 and 24 hrs post treatment (D) indicating that the serine
962 protease gene is involved in the PO pathway. N = 3 (minimum). Mean ± SEM. * $P < 0.05$, ***P
963 < 0.001.

964

965

966

967

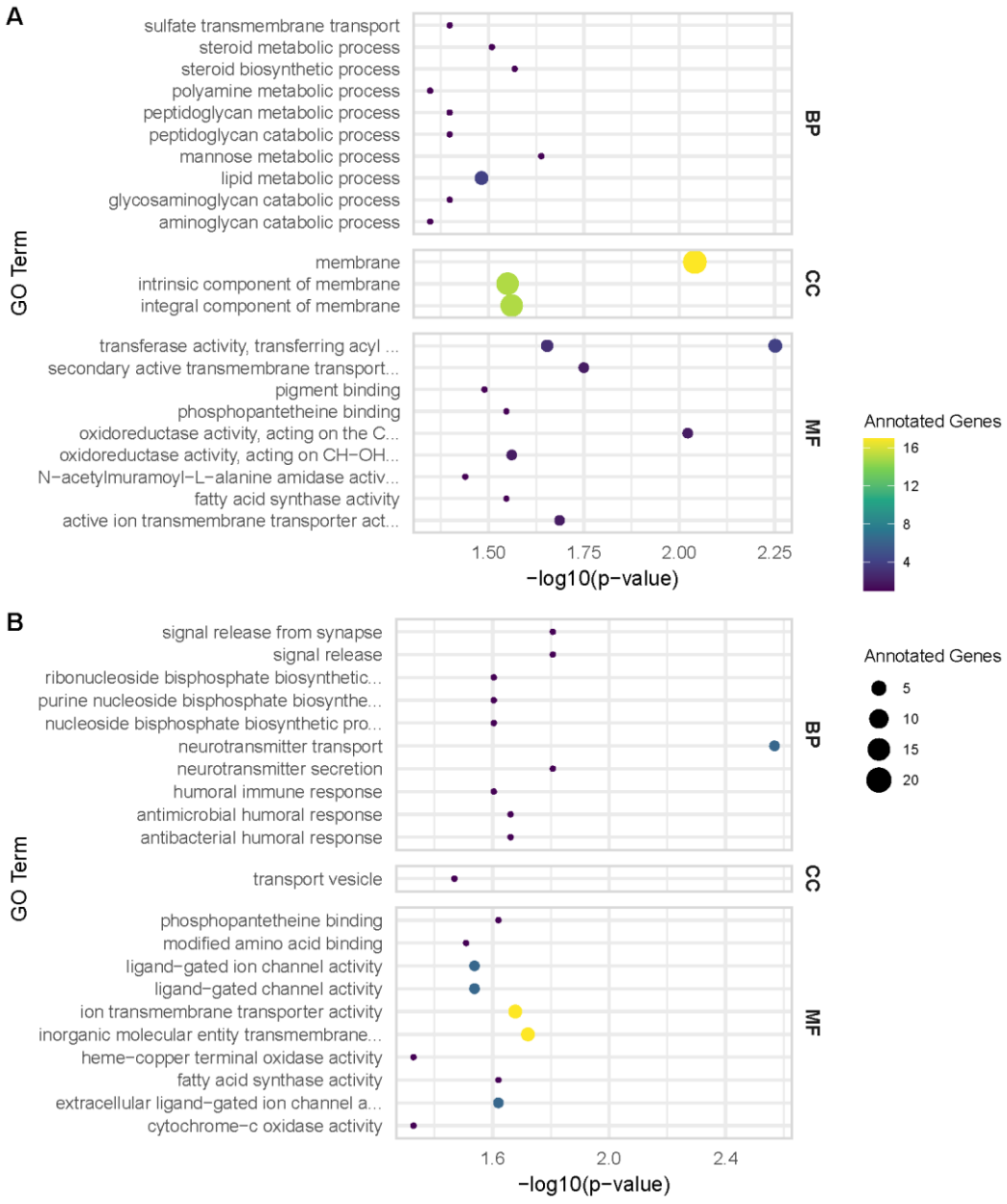

Figure 4. Downregulated mRNAs are involved in signaling and immune responses

GO analysis on significantly upregulated genes (A) shows that these genes are enriched in GO terms associated with metabolic processes and oxidoreductase activity while downregulated genes (B) are enriched for GO terms associated with signaling and immune responses.

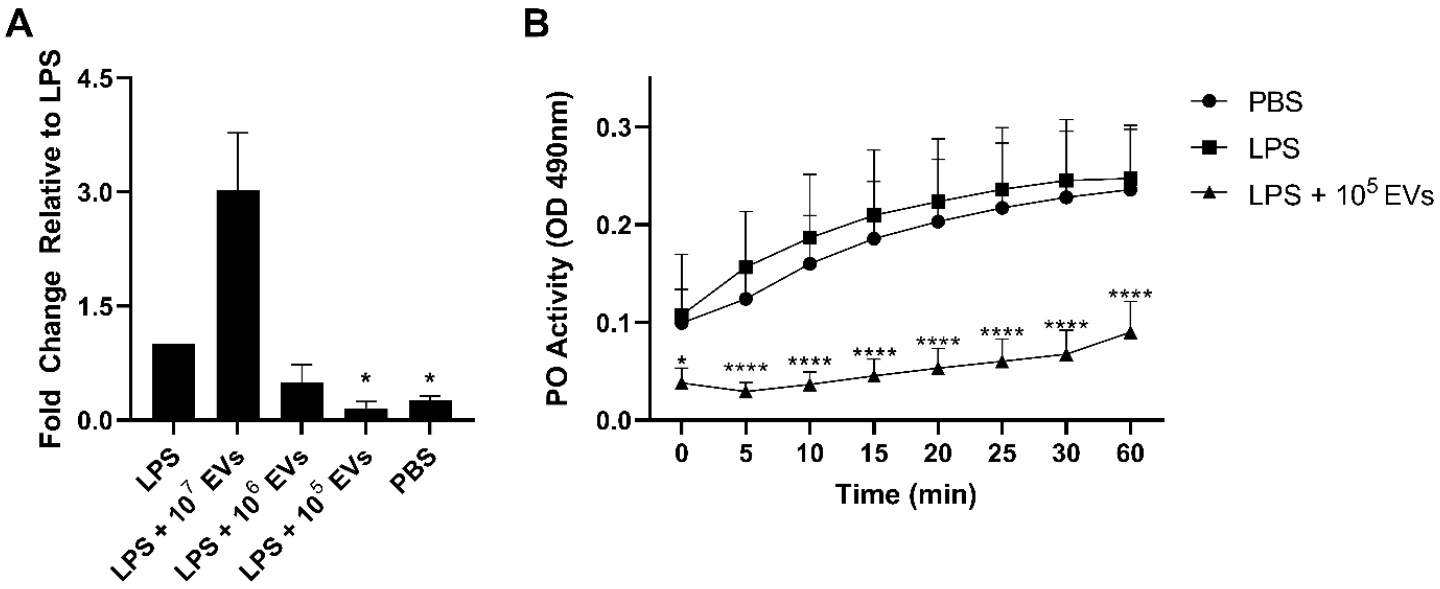

977 **Figure 5. Phenoloxidase activity is inhibited by EV treatment**

978 Validation of the downregulation of the serine protease gene *in vivo* was investigated by
979 injection of adult female mosquitoes with serial dilutions of *B. malayi* mf EVs after initial
980 treatment with LPS. $1x10^5$ EVs significantly downregulated the serine protease gene as
981 compared to LPS only (A). Hemolymph of injected mosquitoes was collected to test for
982 phenoloxidase activity. Treatment of adult female mosquitoes with $1x10^5$ mf EVs inhibited PO
983 activity as compared to LPS only at all time points (B). N = 3 (minimum). Mean ± SEM. *P <
984 0.05, ****P < 0.0001.

985

986

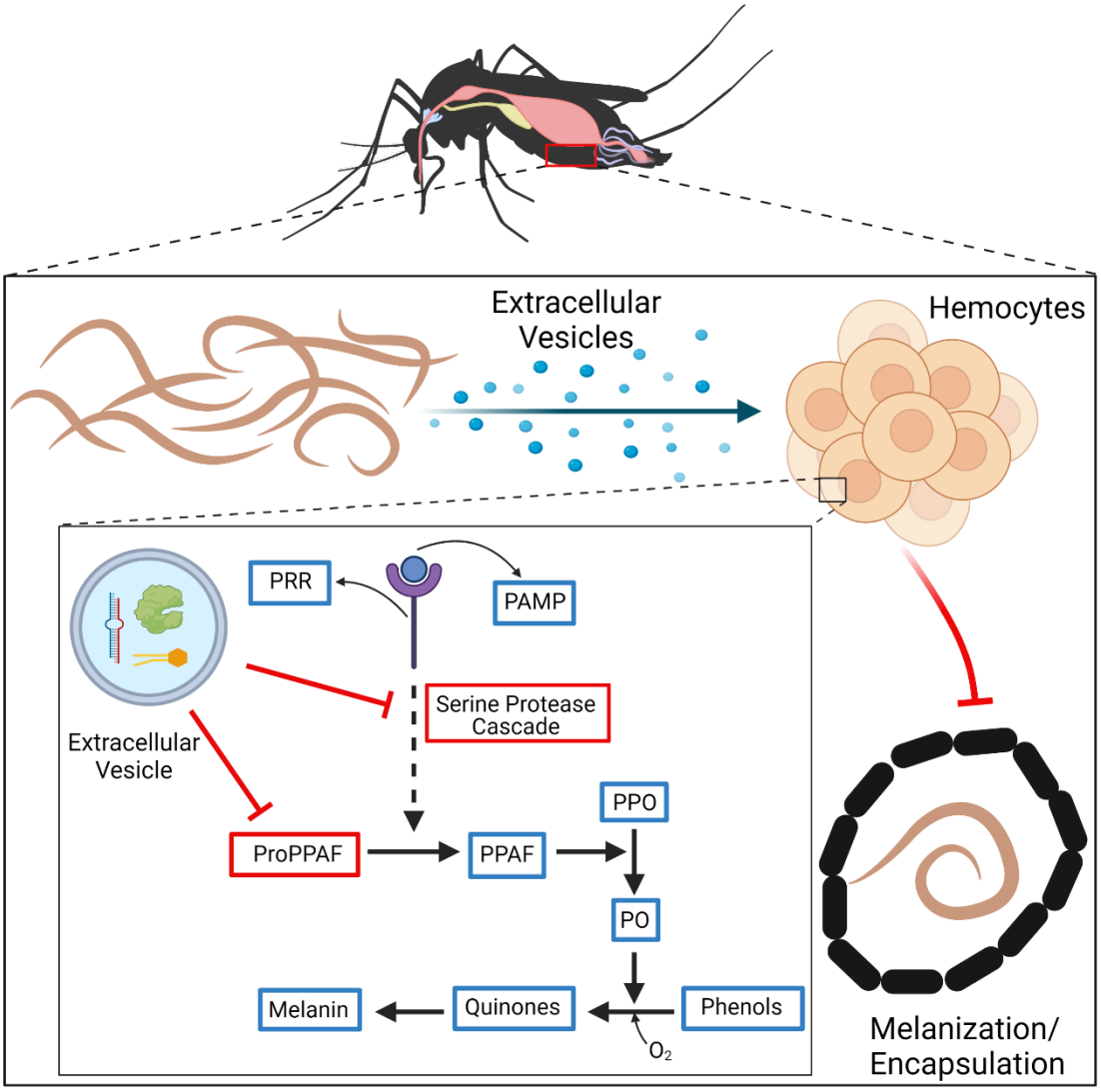

Figure 6. *B. malayi* microfilariae release EVs that interfere with the PO cascade and melanization

Melanotic encapsulation is a common insect defense mechanism against parasites. Upon recognition of a parasite, hemocytes aggregate forming a multicellular layer that deposits a melanin-enriched capsule around the invading parasite. Melanin production is controlled by the phenoloxidase (PO) cascade, which through a series of interdependent reactions, leads to the activation of PO that oxidizes phenols to quinones, which are further polymerized to melanin. Death of the parasite is believed to be due to nutrient deprivation, asphyxiation, or through the production of toxins such as quinones and other reactive oxygen species produced during melanin production. *B. malayi* microfilariae-derived extracellular vesicles downregulate a serine protease that functions either at the serine protease cascade or as a PPAF, either way interfering with the production of PO and thus inhibiting melanization of invading parasites.